Maximizing Network Utility of Rechargeable Sensor Networks With Spatiotemporally Coupled Constraints

Ruilong Deng, *Member, IEEE*, Yongmin Zhang, *Member, IEEE*, Shibo He, *Member, IEEE*, Jiming Chen, *Senior Member, IEEE*, and Xuemin Shen, *Fellow, IEEE*

***Abstract*—This paper studies the network utility maximization (NUM) problem in static-routing rechargeable sensor networks (RSNs) with the link and battery capacity constraints. The NUM problem is very challenging as these two constraints are typically coupling in RSNs, which cannot be directly tackled. Existing works either do not fully consider the two coupled constraints together, or heuristically remove the temporally coupled part, both of which are not practical, and will also degrade the network performance. In this paper, we attempt to jointly optimize the sampling rate and battery level by carefully tackling the spatiotemporally coupled link and battery capacity constraints. To this end, we first decouple the original problem equivalently into separable subproblems by means of dual decomposition. Then, we propose a distributed algorithm in the context of joint rate and battery control, called decouple spatiotemporally-coupled constraint (DSCC), which can converge to the globally optimal solution. Numerical results, based on the real solar data, demonstrate that the proposed algorithm always achieves higher network utility than existing approaches. In addition, the impact of link/battery capacity and initial battery level on the network utility is further investigated.**

***Index Terms*—Dual decomposition, joint rate/battery control, link/battery capacity constraint, network utility maximization, rechargeable sensor network.**

I. Introduction

With the explosive development of microelectronics and wireless communications in recent years, wireless sensor networks (WSNs) have been widely used in a broad range of applications [2]–[7]. Although sensor nodes are low-cost, small-sized and easily-deployed, they are powered by energy-restricted batteries and replacing batteries is infeasible due to the large quantity of nodes. Hence, one critical challenge in WSNs is how to prolong the network lifetime. Recent years have witnessed the emergence of energy harvesting technology to address such an issue — the network lifetime can be potentially extended by harvesting energy from the environment. Known examples of harvestable energy sources for WSNs include solar power [8], electromagnetic waves [9], thermal energy [10], wind [11], vibration [12], etc. The energy harvesting technology opens up a new research area referred to as rechargeable sensor networks (RSNs) [13]–[19].

In general, an RSN is comprised of a number of source nodes that can harvest energy from the environment. Each source samples data and reports them, through some nodes (relays) to the sink. If each source transmits data through fixed relays to the sink, the RSN is referred to as a static-routing RSN. This paper is concerned with the network utility maximization (NUM) problem in static-routing RSNs. There exist two folds of constraints on each source. One is the *link capacity constraint* [20], i.e., the flow over one link should not exceed the link capacity to avoid link congestion. The other is the *battery capacity constraint* [21], i.e., the energy consumption rate should be neither too large nor too small to avoid depletion or overcharge of the rechargeable battery[1]. Taking limited battery capacity into account, two problems emerge: 1) the source depletes the battery and stops working (*aggressive* case); 2) it does not use much energy such that the battery level reaches maximum and misses recharging opportunities (*conservative* case). Obviously, both cases will limit the potential to improve the network utility.

The NUM problem is challenging as the link and battery capacity constraints are typically coupling in RSNs, which cannot be directly tackled. Specifically, in the link capacity constraint, one source's sampling rate is coupled with that of its ancestors (see Eq. (1)). In the battery capacity constraint, to calculate the energy consumption rate, one source's sampling rate is also coupled with that of its ancestors (see Eq. (2)). The reason is that one source needs to relay the sampling rates of its ancestors. Moreover, because the energy consumption rate is constrained by the energy harvesting rate and current battery level to avoid depletion or overcharge of battery, one source's sampling rate is also coupled across the time horizon (see Eq. (7)). Therefore, the NUM problem in static-routing RSNs has the *spatiotemporally-coupled constraints* [1], which, to the best of our knowledge, have not been thoroughly investigated.

Existing works either do not fully consider the coupled link and battery capacity constraints together, or heuristically remove the temporally-coupled part, both of which are not practical in real scenarios, and will also degrade the network

Manuscript received March 12, 2015; revised September 23, 2015; accepted December 4, 2015. Date of publication January 21, 2016; date of current version May 19, 2016. This work was supported in part by NSFC under Grant 61222305, Grant 61004057, Grant 61402405, SRFDP under Grant 20120101110139, NCET-11-0445, and NSERC CRD Grant. A preliminary version of this work was presented at IEEE Globecom 2013 [1].

R. Deng, Y. Zhang, S. He, and J. Chen are with the State Key Laboratory of Industrial Control Technology, Zhejiang University, Hangzhou 310027, China (e-mail: rldeng@iipc.zju.edu.cn; ymzhang@zju.edu.cn; s18he@iipc.zju.edu.cn; jmchen@iipc.zju.edu.cn).

X. Shen is with the Department of Electrical and Computer Engineering, University of Waterloo, Waterloo, ON N2L 3G1, Canada (e-mail: xshen@bbcr.uwaterloo.ca).

Color versions of one or more of the figures in this paper are available online at http://ieeexplore.ieee.org.

Digital Object Identifier 10.1109/JSAC.2016.2520181

[1]The word "battery" in the following text specifically denotes the rechargeable battery.

performance. For example, the energy constraint considered in QuickFix [20] is that the energy consumption rate does not exceed the energy harvesting rate. Without considering the current battery level, such constraints are not coupling across the time horizon, making the problem easier to solve. However, since the excessive harvested energy is not considered to be stored in the battery for later usage, there is no flexibility to allocate the sampling rate evenly among sources and time horizon, and hence the network utility will not be the best. Zhang *et al.* [21] propose an adaptive Energy Allocation sCHeme (EACH), with the energy constraint such that the energy consumption rate does not exceed the energy allocation. Although the energy allocation is based on the energy harvesting rate and current battery level, it is heuristically solved without considering the global optimality. And the remaining problem, without the temporally-coupled part, is then similar to QuickFix. Although EACH improves the network utility a little bit, it still cannot obtain the globally optimal solution. The former work in [1] does not consider the link capacity constraint for congestion control, which is not practical in real scenarios. However, since the link capacity constraint is spatially coupled, incorporating it will add more challenge to the originally complicated problem.

In this paper, we take the attempt to jointly optimize the sampling rate and battery level by carefully tackling the spatiotemporally-coupled link and battery capacity constraints. To this end, we first decouple the original problem equivalently into separable subproblems by means of dual decomposition. Then we propose a distributed algorithm in the context of joint rate and battery control, which can converge to the globally optimal solution. The main contributions are summarized as follows:

1) Both the link and battery capacity constraints are considered to formulate the NUM problem in static-routing RSNs as a spatiotemporally-coupled optimization problem.
2) By carefully tackling the spatiotemporally-coupled constraints through primal-dual approach with strong duality and convergence guarantee, we jointly optimize the sampling rate and battery level, and then propose a distributed algorithm to obtain the globally optimal solution.
3) Numerical results, based on the real solar data, demonstrate that the proposed algorithm always achieves higher network utility than existing approaches. In addition, the impact of link/battery capacity and initial battery level on the network utility is further investigated.

The remainder of this paper is organized as follows. The related works are introduced in Section II. In Section III, we describe the network model and formulate the NUM problem in static-routing RSNs with the link and battery capacity constraints. The problem is dually decomposed into separable subproblems in Section IV. Then in Section V, we propose a distributed algorithm in the context of joint rate and battery control to obtain the globally optimal solution. Numerical results are provided in Section VI, and concluding remarks are drawn in Section VII with future work.

II. Related Works

The problem of optimal energy management, rate allocation and routing in RSNs has drawn considerable attention in recent literatures. For example, Wang *et al.* [22] propose an adaptive data collection and storage system to minimize the sum of all data losses. They also assume that the solar-powered system has the less predicable energy supply and thus needs to adaptively match energy supply and demand. Liu *et al.* [23] study the problem of computing the lexicographically maximum data collection rate and routing paths for perpetual and fair data sensing. They compute the optimal rate when the routing structure is a given tree, and further jointly compute a routing structure and the near-optimal rate. Mao *et al.* [24] study the problem of joint rate control and power allocation to maximize the long-term average sensing rate. They extend from a single communication link to the multi-hop scenario with the near-optimal performance. Gu *et al.* [25] design energy-synchronized communication (ESC) schemes in RSNs to balance energy demand with supply. The ESC scheme acts as a transparent middleware between the network and MAC layers that controls the amount and timing of RF activity at receivers. Different from the above works, this paper is concerned with the NUM problem in RSNs.

There are several works that aim to maximize the network utility in RSNs. For example, Liu *et al.* [20] propose the QuickFix algorithm for computing the data sampling rate and routes, and the SnapIt algorithm to adapt the sampling rate to the battery level. They show that these two algorithms can track the instantaneous optimum network utility while maintaining the battery level at a target value. However, they only consider the energy consumption rate less than the energy harvesting rate instead of the current battery level, let alone the battery capacity constraint. Zhang *et al.* [21] are concerned with how to maximize the overall network performance with limited battery capacity. They develop the EACH algorithm to efficiently manage the battery energy usage, and the DSRC algorithm for obtaining the optimal sampling rate. They further propose the IEACH algorithm to alleviate the impact due to imprecise estimation of energy harvesting. However, they do not consider the link capacity constraint, and the battery capacity constraint is heuristically solved without considering the global optimality. Li *et al.* [26] consider a RSN with a mobile charger and propose to optimize the network utility while guaranteeing sustainability. They include three factors together: uncontrollable ambient energy harvesting, controllable wireless charging, and controllable sensory data generation. However, they do not consider the link capacity constraint, and the proposed distributed scheme is approximate not optimal.

Different from aforementioned works, this paper is concerned with the NUM problem in static-routing RSNs with the link and battery capacity constraints. By carefully tackling the spatiotemporally-coupled link and battery capacity constraints, our goal is to jointly optimize the sampling rate and battery level to further improve the network performance. Besides, the proposed distributed algorithm can converge to the globally optimal solution.

III. Network Model and Problem Formulation

Consider a static-routing RSN with a set $\mathcal{N} \triangleq \{1, \cdots, N\}$ of source nodes. We assume that all nodes are sources except

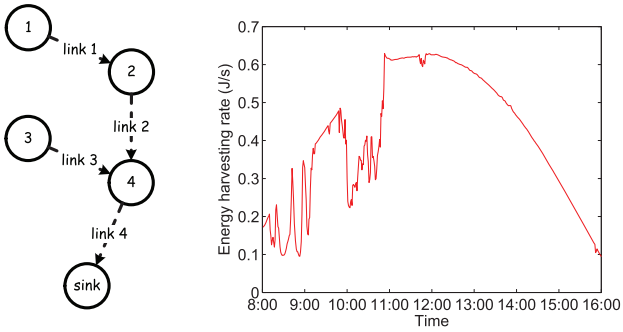

(a) Tree-topology RSN (b) Energy harvesting profile

Fig. 1. Network model.

TABLE I
SUMMARY OF NOTATIONS

Symbol	Definition	Unit[a]
i (or j), $\mathcal{N}$	index of source, set of sources	n/a
$\mathcal{A}$, $\mathcal{R}$	set of ancestors, relays	n/a
h (or t), $\mathcal{H}$	index of time slot, set of time slots	n/a
Δh (or Δt)	duration (granularity) of time slot	s
r, $\boldsymbol{r}$	sampling rate, sampling rate vector	$kbps$
c	link capacity	$kbps$
e^r, e^s, e^t	energy consumption rate for receiving, sampling, transmitting	J/kb
π	energy harvesting rate	J/s
ψ	(comprehensive) energy consumption rate	J/s
δ	missed energy	J
B, B^0, $B^{\max}$	battery level, initial battery level, battery capacity	J
D	energy demand	J
L, U	lower, upper bound of energy constraint	J
$W(\cdot)$	Utility function	n/a
λ, μ, ν	Lagrangian multiplier	n/a
α, β, χ	intermediate variable	n/a
$\boldsymbol{R}$, $\boldsymbol{\Delta}$, $\boldsymbol{\Lambda}$, $\boldsymbol{M}$, $\boldsymbol{N}$	matrix of r, δ, λ, μ, ν	n/a
F, G	rate, battery control subproblem	n/a
γ_λ, γ_μ, γ_ν, θ	step size in iterations of λ, μ, ν, δ	n/a
k	index of iteration	n/a
ε	error tolerance (stopping criterion)	n/a

[a]The unit of a quantity may be omitted in the rest of the paper if it is specified here.

the sink. Each source has a solar photovoltaic panel and a rechargeable battery, so that the excessive harvested energy can be stored in the battery for future usage. The time cycle of energy harvesting is divided into a set $\mathcal{H} \triangleq \{1, \cdots, H\}$ of time slots. In this paper, we consider one day (daytime) as a time cycle, e.g., from 8:00 to 16:00 as shown in Fig. 1(b). If we assume that the duration (granularity) of the time slot is $\Delta h = 10$ min, then the total number of the time slots is $H = 48$. The other days could repeat the same way. Since this work mainly focuses on joint rate and battery control to maximize network utility of RSNs, the channel model and link scheduling can be referred to the existing literatures [20]–[26]. Some important notations used in this paper are summarized in TABLE I. In the rest of this work, we also use the following mathematical notations: $\boldsymbol{x}^T$ denotes the transpose of $\boldsymbol{x}$; $\|\boldsymbol{x}\|_2$ denotes the $\mathcal{L}_2$ (Euclidean) norm of $\boldsymbol{x}$; $[\cdot]^+$ denotes $\max\{\cdot, 0\}$; $[\cdot]_a^b$ denotes $\min\{\max\{\cdot, a\}, b\}$; $f'(\cdot)$ denotes the first derivative of function $f(\cdot)$; and $f^{-1}(\cdot)$ denotes the inverse of function $f(\cdot)$.

A. Link Capacity Constraint

In the static-routing RSN, we assume a tree topology with single-path routing. At each time slot $h \in \mathcal{H}$, each source $i \in \mathcal{N}$ samples data at rate r_i^h, and emits one flow, through a fixed set $\mathcal{R}(i)$ of relays to the sink. Each source $i \in \mathcal{N}$ has only one link to its next hop, with limited link capacity c_i^h, which is variant at each time slot $h \in \mathcal{H}$. Taking the tree-topology RSN in Fig. 1(a) for example, $\mathcal{R}(1) = \{2, 4\}$, i.e., one source's relays are the downstream nodes of that source. Let $\mathcal{A}(i) \triangleq \{j | i \in \mathcal{R}(j)\}$ denote the set of ancestors who use the source i as a relay. Taking the tree-topology RSN in Fig. 1(a) for example, $\mathcal{A}(4) = \{1, 2, 3\}$, i.e., one source's ancestors are the upstream nodes of that source. Thus the link capacity constraint of each source is

$$r_i^h + \sum_{j \in \mathcal{A}(i)} r_j^h \le c_i^h, \tag{1}$$

which indicates that the flow over one link should not exceed the link capacity to avoid link congestion. In the link capacity constraint, one source's sampling rate is coupled with that of its ancestors.

B. Battery Capacity Constraint

At each time slot $h \in \mathcal{H}$, let π_i^h denote the source i's energy harvesting rate, which is assumed to be predicted and estimated with high accuracy [27], taking the energy harvesting profile in Fig. 1(b) for example. Each source consumes energy for sensing and communication (including data reception and transmission). Let e_i^r, e_i^s, and e_i^t denote the source i's energy consumption rates for receiving, sampling, and transmitting, respectively. $\boldsymbol{r}^h \triangleq \left[r_1^h, \cdots, r_N^h\right]^T$ is the sampling rate vector. The (comprehensive) energy consumption rate of each source is defined by

$$\psi_i\left(\boldsymbol{r}^h\right) \triangleq \left(e_i^s + e_i^t\right) r_i^h + \left(e_i^r + e_i^t\right) \sum_{j \in \mathcal{A}(i)} r_j^h, \tag{2}$$

where one source's sampling rate is coupled with that of its ancestors.

Let B_i^h denote the source i's battery level at the end of the time slot h, which is calculated by

$$B_i^h = \left[B_i^{h-1} + \pi_i^h \Delta h - \psi_i\left(\boldsymbol{r}^h\right) \Delta h\right]_0^{B_i^{\max}}, \tag{3}$$

where Δh indicates the duration (granularity) of the time slot h, and $B_i^{\max}$ denotes the source i's battery capacity. For the ease of presentation, define a surplus variable [21], [23]

$$\delta_i^h \triangleq \left[B_i^{h-1} + \pi_i^h \Delta h - \psi_i\left(\boldsymbol{r}^h\right) \Delta h - B_i^{\max}\right]^+$$

as "missed energy", whose physical meaning is the amount of the harvested energy that cannot be stored in the source i's battery at the time slot h if the battery is full. If the source i's battery at the time slot h is not full, then $\delta_i^h = 0$. Thus the actual amount of the harvested energy that can be stored in the source

i's battery at the time slot h is $\pi_i^h \Delta h - \delta_i^h$. By use of δ_i^h, Eq. (3) can be recursively calculated by

$$\begin{aligned} B_i^h &= B_i^{h-1} + \pi_i^h \Delta h - \psi_i\left(\boldsymbol{r}^h\right)\Delta h - \delta_i^h \\ &= B_i^0 + \sum_{t=1}^{h} \pi_i^t \Delta t - \sum_{t=1}^{h} \psi_i\left(\boldsymbol{r}^t\right)\Delta t - \sum_{t=1}^{h} \delta_i^t, \end{aligned} \tag{4}$$

where the source i's initial battery level B_i^0 is assumed to be known.

With limited battery capacity, the energy consumption rate of each source[2] is constrained by

$$0 \le B_i^h = B_i^{h-1} + \pi_i^h \Delta h - \psi_i\left(\boldsymbol{r}^h\right)\Delta h - \delta_i^h \le B_i^{\max}, \tag{5}$$

which indicates that the energy consumption rate should be neither too large such that the source depletes the battery and stops working (aggressive case), nor too small such that the battery level reaches maximum and misses recharging opportunities (conservative case). Note that since $\delta_i^h \ge 0$, we have $B_i^{h-1} + \pi_i^h \Delta h - \psi_i\left(\boldsymbol{r}^h\right)\Delta h \ge \delta_i^h \ge 0$, i.e., each source must have enough energy to support the sampling rate at each time slot.

By substituting Eq. (4) for B_i^h, Eq. (5) is rewritten as

$$0 \le B_i^h = B_i^0 + \sum_{t=1}^{h} \pi_i^t \Delta t - \sum_{t=1}^{h} \left[\psi_i\left(\boldsymbol{r}^t\right)\Delta t + \delta_i^t\right] \le B_i^{\max}.$$

For simplicity, we define a variable

$$D_i^t\left(\boldsymbol{r}^t, \delta_i^t\right) \triangleq \psi_i\left(\boldsymbol{r}^t\right)\Delta t + \delta_i^t \tag{6}$$

as the source i's energy demand at the time slot t, and two constants

$$\begin{cases} L_i^h \triangleq U_i^h - B_i^{\max} \\ U_i^h \triangleq B_i^0 + \sum\limits_{t=1}^{h} \pi_i^t \Delta t \end{cases}$$

to be the lower and upper bounds of the energy constraint, respectively. Thus the battery capacity constraint of each source is

$$L_i^h \le \sum_{t=1}^{h} D_i^t\left(\boldsymbol{r}^t, \delta_i^t\right) \le U_i^h, \tag{7}$$

where one source's sampling rate is also coupled across the time horizon.

C. Problem Formulation

The source i attains utility $W\left(r_i^h\right)$ when it samples data at rate r_i^h at the time slot h, where the utility can be a specific performance (e.g., data gathering) required by applications. The utility function $W(\cdot)$ is assumed to be increasing and strictly concave [21]. For example, let $W\left(r_i^h\right) \triangleq \log\left(r_i^h\right)$, which is known to guarantee the fairness of each source. The NUM problem in static-routing RSNs with the link and battery capacity constraints is to maximize the network utility $\sum_{h\in\mathcal{H}}\sum_{i\in\mathcal{N}} W\left(r_i^h\right)$ over the sampling rate matrix $\boldsymbol{R} \triangleq \left[r_i^h\right]_{i\in\mathcal{N},h\in\mathcal{H}}$ and missed energy matrix $\boldsymbol{\Delta} \triangleq \left[\delta_i^h\right]_{i\in\mathcal{N},h\in\mathcal{H}}$, under the link capacity constraint (1) and battery capacity constraint (7):

Primal Problem:

$$\begin{aligned} \max_{\boldsymbol{R},\boldsymbol{\Delta}} \quad & \sum_{h\in\mathcal{H}}\sum_{i\in\mathcal{N}} W\left(r_i^h\right) \\ \text{s.t.} \quad & \begin{cases} (1) \text{ and } (7) \\ r_i^h, \delta_i^h \ge 0 \end{cases} \quad \forall i \in \mathcal{N},\ \forall h \in \mathcal{H}. \end{aligned} \tag{8}$$

IV. Dual Decomposition

With the coupled link and battery capacity constraints (1) and (7), especially the spatiotemporally-coupled constraint (7) which couples one source's sampling rate with that of its ancestors across the time horizon, the primal problem (8) cannot be directly tackled. However, by means of dual decomposition [28]–[32], we can decouple the original problem equivalently into separable subproblems and then solve them locally. Due to strong duality, the primal problem and its dual problem are equivalent.

A. Lagrangian

Define the Lagrangian

$$\begin{aligned} \mathscr{L}\left(\boldsymbol{R}, \boldsymbol{\Delta}, \boldsymbol{\Lambda}, \boldsymbol{M}, \boldsymbol{N}\right) &= \sum_{h\in\mathcal{H}}\sum_{i\in\mathcal{N}} W\left(r_i^h\right) \\ &+ \sum_{h\in\mathcal{H}}\sum_{i\in\mathcal{N}} \left\{ \lambda_i^h \left[\sum_{t=1}^{h} D_i^t\left(\boldsymbol{r}^t, \delta_i^t\right) - L_i^h\right] \right. \\ &+ \mu_i^h \left[U_i^h - \sum_{t=1}^{h} D_i^t\left(\boldsymbol{r}^t, \delta_i^t\right)\right] \\ &\left. + \nu_i^h \left[c_i^h - \left(r_i^h + \sum_{j\in\mathcal{A}(i)} r_j^h\right)\right]\right\}, \end{aligned}$$

where we relax the coupled constraints (1) and (7), respectively, by introducing the Lagrangian multipliers $\lambda_i^h, \mu_i^h, \nu_i^h \ge 0$ for each source at each time slot, and $\boldsymbol{\Lambda} \triangleq \left[\lambda_i^h\right]_{i\in\mathcal{N},h\in\mathcal{H}}$, $\boldsymbol{M} \triangleq \left[\mu_i^h\right]_{i\in\mathcal{N},h\in\mathcal{H}}$, and $\boldsymbol{N} \triangleq \left[\nu_i^h\right]_{i\in\mathcal{N},h\in\mathcal{H}}$ are the Lagrangian multiplier matrixes. Note that

$$\begin{cases} \sum\limits_{h\in\mathcal{H}} \left[\left(\lambda_i^h - \mu_i^h\right)\sum\limits_{t=1}^{h} D_i^t\right] = \sum\limits_{h\in\mathcal{H}} \left[\psi_i\left(\boldsymbol{r}^h\right)\Delta h + \delta_i^h\right]\alpha_i^h \\ \sum\limits_{i\in\mathcal{N}} \psi_i\left(\boldsymbol{r}^h\right)\Delta h \cdot \alpha_i^h = \sum\limits_{i\in\mathcal{N}} r_i^h \beta_i^h \\ \sum\limits_{i\in\mathcal{N}} \nu_i^h \left(r_i^h + \sum\limits_{j\in\mathcal{A}(i)} r_j^h\right) = \sum\limits_{i\in\mathcal{N}} r_i^h \chi_i^h, \end{cases}$$

[2]The sink is assumed to connect with an electrical wire, and thus there is no need to consider the energy constraint on it.

if we define the intermediate variables

$$\begin{cases} \alpha_i^h \triangleq \sum_{t=h}^{H} \left(\lambda_i^t - \mu_i^t\right) & \text{(9a)} \\ \beta_i^h \triangleq \left[\alpha_i^h \left(e_i^s + e_i^t\right) + \sum_{j\in\mathcal{R}(i)} \alpha_j^h \left(e_j^r + e_j^t\right)\right] \Delta h & \text{(9b)} \\ \chi_i^h \triangleq \nu_i^h + \sum_{j\in\mathcal{R}(i)} \nu_j^h. & \text{(9c)} \end{cases}$$

These equations can be proved through expansion of both sides and mathematical induction. Thus the Lagrangian is

$$\begin{aligned} &\mathscr{L}\left(\boldsymbol{R}, \boldsymbol{\Delta}, \boldsymbol{\Lambda}, \boldsymbol{M}, \boldsymbol{N}\right) = \\ &\sum_{h\in\mathcal{H}} \sum_{i\in\mathcal{N}} \left[W\left(r_i^h\right) + \left(\beta_i^h - \chi_i^h\right) r_i^h + \alpha_i^h \delta_i^h\right] \\ &+ \sum_{h\in\mathcal{H}} \sum_{i\in\mathcal{N}} \left(-\lambda_i^h L_i^h + \mu_i^h U_i^h + \nu_i^h c_i^h\right). \end{aligned}$$

B. Subproblem and Dual Problem

The dual function is the maximum value of the Lagrangian over the system variables $\boldsymbol{R}$ and $\boldsymbol{\Delta}$:

$$\mathscr{D}\left(\boldsymbol{\Lambda}, \boldsymbol{M}, \boldsymbol{N}\right) = \sup_{\boldsymbol{R}, \boldsymbol{\Delta}} \mathscr{L}\left(\boldsymbol{R}, \boldsymbol{\Delta}, \boldsymbol{\Lambda}, \boldsymbol{M}, \boldsymbol{N}\right).$$

Define

Subproblem:

$$\begin{cases} F_i^h\left(\boldsymbol{\Lambda}, \boldsymbol{M}, \boldsymbol{N}\right) \triangleq \max_{r_i^h \geq 0} \left[W\left(r_i^h\right) + \left(\beta_i^h - \chi_i^h\right) r_i^h\right] & \text{(10a)} \\ G_i^h\left(\boldsymbol{\Lambda}, \boldsymbol{M}\right) \triangleq \max_{\delta_i^h \geq 0} \alpha_i^h \delta_i^h & \text{(10b)} \end{cases}$$

as the $(i, h)^{\text{th}}$ Lagrangian to be maximized by the source i at the time slot h. Thus the dual function is

$$\begin{aligned} \mathscr{D}\left(\boldsymbol{\Lambda}, \boldsymbol{M}, \boldsymbol{N}\right) = &\sum_{h\in\mathcal{H}} \sum_{i\in\mathcal{N}} \left[F_i^h\left(\boldsymbol{\Lambda}, \boldsymbol{M}, \boldsymbol{N}\right) + G_i^h\left(\boldsymbol{\Lambda}, \boldsymbol{M}\right)\right] \\ &+ \sum_{h\in\mathcal{H}} \sum_{i\in\mathcal{N}} \left(-\lambda_i^h L_i^h + \mu_i^h U_i^h + \nu_i^h c_i^h\right). \end{aligned}$$

The dual problem is to minimize the dual function over the Lagrangian multipliers $\boldsymbol{\Lambda}$ and $\boldsymbol{M}$:

Dual Problem:

$$\begin{aligned} \min_{\boldsymbol{\Lambda}, \boldsymbol{M}, \boldsymbol{N}} \quad & \mathscr{D}\left(\boldsymbol{\Lambda}, \boldsymbol{M}, \boldsymbol{N}\right) \qquad \text{(11)} \\ \text{s.t.} \quad & \lambda_i^h, \mu_i^h, \nu_i^h \geq 0 \quad \forall i \in \mathcal{N}, \ \forall h \in \mathcal{H}. \end{aligned}$$

The dual problem (11) can be iteratively solved using the subgradient projection method, and the Lagrangian multipliers are updated in an opposite direction to the subgradient of the dual function:

$$\begin{cases} \lambda_i^{h,k+1} = \left[\lambda_i^{h,k} - \gamma_\lambda \nabla_{\lambda_i^h} \mathscr{D}\right]^+ \\ \mu_i^{h,k+1} = \left[\mu_i^{h,k} - \gamma_\mu \nabla_{\mu_i^h} \mathscr{D}\right]^+ \\ \nu_i^{h,k+1} = \left[\nu_i^{h,k} - \gamma_\nu \nabla_{\nu_i^h} \mathscr{D}\right]^+, \end{cases}$$

where γ_λ, γ_μ, and $\gamma_\nu > 0$ are the step sizes which adjust the convergence rate, and $k \in \mathbb{N}^+$ denotes the index of iteration.

Theorem 1: The primal problem (8) has strong duality.

Proof: First, the primal problem (8) is the maximization over a concave function, which is equivalent to the minimization over a convex function. Then, the inequality constraint functions (1) and (7) are affine. It is proved in [28, Sec. 5.3.2] that strong duality holds since (8) satisfies the constraint qualification. ■

With strong duality, the optimal duality gap is zero. Therefore, to solve the primal problem (8) is equivalent to solving its dual problem (11).

V. Solution

A. Subproblem Solution

By means of dual decomposition, the global optimization problem (8) has been equivalently decoupled into separable local optimization subproblems (10a) and (10b) at each source at each time slot. One subproblem (10a) corresponds to *rate control* — to determine the optimal sampling rate. The other subproblem (10b) is *battery control* — to calculate the missed energy due to limited battery capacity. We solve these subproblems in the context of joint rate and battery control.

1) Rate control: for the subproblem (10a) at each source at each time slot, given $\boldsymbol{\Lambda}^k$, $\boldsymbol{M}^k$, and $\boldsymbol{N}^k$, the sampling rate

$$\tilde{r}_i^h = \left[\left(W'\right)^{-1}\left(\chi_i^{h,k} - \beta_i^{h,k}\right)\right]^+ \qquad \text{(12)}$$

is unique due to the strict concavity of $W(\cdot)$. Besides, the function $\left(W'\right)^{-1}(\cdot)$ is monotonely decreasing. Under arbitrary $\boldsymbol{\Lambda}^k$, $\boldsymbol{M}^k$, and $\boldsymbol{N}^k$, the local maximizer $\tilde{r}_i^h$ may not be globally optimal. However, by duality theory, there exists dual optimal $\boldsymbol{\Lambda}^*$, $\boldsymbol{M}^*$, and $\boldsymbol{N}^*$ such that r_i^{h*} will be globally optimal.

2) Battery control: for the subproblem (10b) at each source at each time slot, given $\boldsymbol{\Lambda}^k$ and $\boldsymbol{M}^k$, the missed energy can be iteratively solved using the gradient projection method:

$$\tilde{\delta}_i^h = \left[\tilde{\delta}_i^h + \theta \alpha_i^{h,k}\right]^+, \qquad \text{(13)}$$

where $\theta > 0$ is the step size which adjusts the convergence rate.

From the above, given $\boldsymbol{\Lambda}^*$, $\boldsymbol{M}^*$, and $\boldsymbol{N}^*$ from the dual problem (11), each source can solve the subproblems (10a) and (10b) *locally without the need to coordinate with other sources or time slots*. In such sense, the Lagrangian multipliers serve as coordination signals which align the local optimality of (10a) and (10b) with the global optimality of (8).

B. Dual Problem Solution

Recall that the subproblems (10a) and (10b) have the local optimal solutions $\tilde{r}_i^h$ and $\tilde{\delta}_i^h$ respectively. Thus we have

$$\begin{cases} F_i^h\left(\boldsymbol{\Lambda}, \boldsymbol{M}, \boldsymbol{N}\right) = W\left(\tilde{r}_i^h\right) + \left(\beta_i^h - \chi_i^h\right) \tilde{r}_i^h \\ G_i^h\left(\boldsymbol{\Lambda}, \boldsymbol{M}\right) = \alpha_i^h \tilde{\delta}_i^h, \end{cases}$$

and

$$\begin{cases} \nabla_{\lambda_i^h}\mathscr{D} = \sum_{t=1}^{h} D_i^t\left(\tilde{\boldsymbol{r}}^t, \tilde{\delta}_i^t\right) - L_i^h \\ \nabla_{\mu_i^h}\mathscr{D} = U_i^h - \sum_{t=1}^{h} D_i^t\left(\tilde{\boldsymbol{r}}^t, \tilde{\delta}_i^t\right) \\ \nabla_{\nu_i^h}\mathscr{D} = c_i^h - \left(\tilde{r}_i^h + \sum_{j\in\mathcal{A}(i)} \tilde{r}_j^h\right). \end{cases}$$

We obtain the following Lagrangian multiplier update rules:

$$\lambda_i^{h,k+1} = \left\{\lambda_i^{h,k} - \gamma_\lambda\left[\sum_{t=1}^{h} D_i^t\left(\tilde{\boldsymbol{r}}^t, \tilde{\delta}_i^t\right) - L_i^h\right]\right\}^+ \quad (14a)$$

$$\mu_i^{h,k+1} = \left\{\mu_i^{h,k} - \gamma_\mu\left[U_i^h - \sum_{t=1}^{h} D_i^t\left(\tilde{\boldsymbol{r}}^t, \tilde{\delta}_i^t\right)\right]\right\}^+ \quad (14b)$$

$$\nu_i^{h,k+1} = \left\{\nu_i^{h,k} - \gamma_\nu\left[c_i^h - \left(\tilde{r}_i^h + \sum_{j\in\mathcal{A}(i)} \tilde{r}_j^h\right)\right]\right\}^+, \quad (14c)$$

which indicates, if the source's accumulated energy demand $\sum_{t=1}^{h} D_i^t\left(\tilde{\boldsymbol{r}}^t, \tilde{\delta}_i^t\right)$ is less than the lower bound L_i^h (conservative case), λ_i^h will rise, increasing α_i^h and β_i^h, which will in turn increase the sampling rate r_i^h and missed energy δ_i^h; however, if it exceeds the upper bound U_i^h (aggressive case), μ_i^h will rise, decreasing α_i^h and β_i^h, which will in turn decrease the sampling rate r_i^h and missed energy δ_i^h. On the other hand, the Lagrangian multiplier ν_i^h can be interpreted as the link congestion price, which indicates, if at time slot h the flow $\tilde{r}_i^h + \sum_{j\in\mathcal{A}(i)} \tilde{r}_j^h$ over link i exceeds the link capacity c_i^h, the link congestion price ν_i^h will rise, increasing χ_i^h, which will in turn decrease the sampling rate r_i^h to avoid link congestion, and vice versa.

C. Distributed Algorithm

Let $\mathcal{NA}(i)$ denote the set of the neighbor ancestors of the source i, and $NR(i)$ for the neighbor relay of the source i. Taking the tree-topology RSN in Fig. 1(a) for example, $\mathcal{NA}(4) = \{2, 3\}$ and $NR(1) = 2$. At each time slot $h \in \mathcal{H}$, let $R_i^h \triangleq r_i^h + \sum_{j\in\mathcal{A}(i)} r_j^h$ denote the sum of the sampling rates that the source i needs to transmit, which can be expressed in a recursive way as

$$R_i^h = r_i^h + \sum_{j\in\mathcal{NA}(i)} R_j^h. \quad (15)$$

Then Eq. (2) and Eq. (14c) can be rewritten as

$$\psi_i\left(\boldsymbol{r}^h\right) \triangleq \left(e_i^s + e_i^t\right) r_i^h + \left(e_i^r + e_i^t\right)\left(R_i^h - r_i^h\right), \quad (16)$$

and

$$\nu_i^{h,k+1} = \left[\nu_i^{h,k} - \gamma_\nu\left(c_i^h - \tilde{R}_i^h\right)\right]^+. \quad (17)$$

Similarly, if we at the same time denote $A_i^h \triangleq \alpha_i^h\left(e_i^s + e_i^t\right) + \sum_{j\in\mathcal{R}(i)} \alpha_j^h\left(e_j^r + e_j^t\right)$ in a recursive way as

$$A_i^h = \alpha_i^h\left(e_i^s + e_i^t\right) + \tilde{A}_{NR(i)}^h, \quad (18)$$

where

$$\tilde{A}_{NR(i)}^h \triangleq A_{NR(i)}^h + \alpha_{NR(i)}^h\left(e_{NR(i)}^r - e_{NR(i)}^s\right), \quad (19)$$

then Eq. (9b) can be rewritten as

$$\beta_i^h \triangleq A_i^h \Delta h. \quad (20)$$

Similarly, Eq. (9c) can be expressed in a recursive way as

$$\chi_i^h \triangleq \nu_i^h + \chi_{NR(i)}^h. \quad (21)$$

Algorithm 1. DSCC

Input: network topology and configuration, energy consumption rate and energy harvesting profile, link/battery capacity and initial battery level
Output: sampling rate $\boldsymbol{R}^*$ and missed energy $\boldsymbol{\Delta}^*$

Initialization: $k \leftarrow 1$, each source $i \in \mathcal{N}$ begins with arbitrary nonnegative Lagrangian multipliers $\left\{\lambda_i^{h,1}\right\}_{h\in\mathcal{H}}$, $\left\{\mu_i^{h,1}\right\}_{h\in\mathcal{H}}$, and $\left\{\nu_i^{h,1}\right\}_{h\in\mathcal{H}}$;
repeat
  for *each source* $i = N, \cdots, 1$ **do**
    receives $\left\{\tilde{A}_{NR(i)}^{h,k}\right\}_{h\in\mathcal{H}}$ and $\left\{\chi_{NR(i)}^{h,k}\right\}_{h\in\mathcal{H}}$ from its neighbor relay $NR(i)$;
    for *each time slot* $h = H, \cdots, 1$ **do**
      calculates $\alpha_i^{h,k}$, $A_i^{h,k}$, $\tilde{A}_i^{h,k}$, $\beta_i^{h,k}$, and $\chi_i^{h,k}$ from (9a), (18), (19), (20), and (21);
      computes $\tilde{r}_i^h$ and $\tilde{\delta}_i^h$ from (12) and (13);
    end for
    sends $\left\{\tilde{A}_i^{h,k}\right\}_{h\in\mathcal{H}}$ and $\left\{\chi_i^{h,k}\right\}_{h\in\mathcal{H}}$ to all its neighbor ancestors $\mathcal{NA}(i)$;
  end for
  for *each source* $i = 1, \cdots, N$ **do**
    receives $\left\{\tilde{R}_j^h\right\}_{h\in\mathcal{H}}$ from all its neighbor ancestors $j \in \mathcal{NA}(i)$;
    for *each time slot* $h = 1, \cdots, H$ **do**
      calculates $\tilde{R}_i^h$, $\psi_i\left(\tilde{\boldsymbol{r}}^h\right)$, and $\sum_{t=1}^{h} D_i^t\left(\tilde{\boldsymbol{r}}^t, \tilde{\delta}_i^t\right)$ from (15), (16), and (6);
      updates $\lambda_i^{h,k+1}$, $\mu_i^{h,k+1}$, and $\nu_i^{h,k+1}$ from (14a), (14b), and (17);
    end for
    sends $\left\{\tilde{R}_i^h\right\}_{h\in\mathcal{H}}$ to its neighbor relay $NR(i)$;
  end for
  $k \leftarrow k + 1$;
until $\boldsymbol{\Lambda}$, $\boldsymbol{M}$, *and* $\boldsymbol{N}$ *converge within a small range* ε;

From the discussion in the previous section, each source can be treated as processors in the distributed computation system to solve the NUM problem in static-routing RSNs with the link and battery capacity constraints. Assume that all source nodes are indexed in descending order of their hop counts to the sink, taking the tree-topology RSN in Fig. 1(a) for

example. We propose a distributed algorithm (**Algorithm 1**) in the context of joint rate and battery control, called Decouple Spatiotemporally-Coupled Constraint (DSCC), which can converge to the globally optimal solution. Each iteration includes two rounds. In the first round, each source $i = N, \cdots, 1$ from bottom (root) to top (leaf) locally computes its sampling rate $\tilde{r}_i^h$ and missed energy $\tilde{\delta}_i^h$ (line 7), based on the information from its neighbor relay (line 4). Specifically, once a source receives message from its neighbor relay, it performs local computing, and then sends message to all its neighbor ancestors. The process goes so on and so forth, from bottom (root) to top (leaf). Similarly, in the second round, each source $i = 1, \cdots, N$ from top (leaf) to bottom (root) locally updates its Lagrangian multipliers $\lambda_i^{h,k+1}$, $\mu_i^{h,k+1}$, and $\nu_i^{h,k+1}$ (line 15), based on the information from all its neighbor ancestors (line 12). Specifically, once a source receives message from all its neighbor ancestors, it performs local computing, and then sends message to its neighbor relay. The process goes so on and so forth, from top (leaf) to bottom (root). From the above, synchronization is not needed for iterations. To deal with lost message, besides waiting for retransmission, an alternative way is to use the former message received in the previous iteration. The cycle repeats until all Lagrangian multipliers converge within a small range ε, which indicates the error tolerance (stopping criterion) to stop the calculation. The overhead is the neighborhood communication with a few control messages to exchange. DSCC is a low-cost algorithm, as neighbor sources collaborate with each other to adjust their sampling rates and missed energies in a distributed manner. The amount of communication overhead is relatively small, compared to that of one day's sampling data. Besides, since the algorithm performs only once at the beginning of the time cycle (one day), compared to the amount of battery capacity and one day's energy harvesting, the energy consumption has relatively small impact on the problem investigated.

Theorem 2: With the sufficiently small step sizes γ_λ, γ_μ, and γ_ν, the DSCC algorithm converges to the globally optimal sampling rate $\boldsymbol{R}^*$ and missed energy $\boldsymbol{\Delta}^*$, as long as the primal problem (8) is feasible.

Proof: We define the single Lagrangian multiplier $\boldsymbol{\Omega} \triangleq [\boldsymbol{\Lambda}, \boldsymbol{M}, \boldsymbol{N}]$. Since the utility function $W(\cdot)$ is strictly concave, and thus the relationship from the sampling rate $\boldsymbol{R}$ and missed energy $\boldsymbol{\Delta}$ to the Lagrangian multiplier $\boldsymbol{\Omega}$ is monotone, there exist the sufficiently small step sizes γ_λ, γ_μ, and γ_ν that guarantee the convergence of the subgradient projection method [33]. The DSCC algorithm converges when $0 < \gamma_\lambda, \gamma_\mu$, and $\gamma_\nu < 2/K$, where K is the Lipschitz constant for the dual function:

$$\|\nabla \mathscr{D}(\boldsymbol{\Omega}_1) - \nabla \mathscr{D}(\boldsymbol{\Omega}_2)\|_2 \leq K \|\boldsymbol{\Omega}_1 - \boldsymbol{\Omega}_2\|_2 .$$

■

VI. Numerical Results

A. Simulation Setup

In this section, we provide numerical results to demonstrate the performance of the proposed algorithm. Consider an RSN comprised of four source nodes, with the network topology shown in Fig. 1(a) [21], [23], where the node (link) 4 is the bottleneck node (link). Each source has a $37 \times 33\ mm^2$ solar photovoltaic panel, and a super capacitor as the rechargeable battery, whose capacity is $304\ J$. Besides, each source has a wireless transceiver module such as Telos [34], and the energy consumption rates for receiving, sampling, and transmitting are $0.069\ J/kb$, $0.0054\ J/kb$, and $0.063\ J/kb$, respectively [21], [23]. We use the real solar data collected from the Baseline Measurement System at the NREL Solar Radiation Research Laboratory [35]. For example, the data at noon on December 12, 2012 is $512\ W/m^2$, so the energy harvesting rate at that time is $0.625\ J/s$, as shown by the energy harvesting profile in Fig. 1(b)[3]. Assume that the initial battery level of each source is zero. Let the utility function be $W\left(r_i^h\right) \triangleq \log\left(r_i^h\right)$, which is known to guarantee the fairness of each source. The above simulation parameters are summarized in TABLE II for reference. All the following results are obtained by MATLAB R2007b running on a laptop PC with Intel Core i5-3320 CPU @ 2.6 GHz, 4 GB RAM memory, and 32-bit Windows 7 OS.

TABLE II
Parameter Setting

Parameter	Value	Parameter	Value
e^r	$0.069\ J/kb$	$B^{\max}$	$304\ J$
e^s	$0.0054\ J/kb$	B^0	$0\ J$
e^t	$0.063\ J/kb$	ε	10^{-3}

B. Performance Comparison

We first compare DSCC with QuickFix [20], whose energy constraint is that the energy consumption rate does not exceed the energy harvesting rate. The simulation results of DSCC and QuickFix are shown in Fig. 2(a) and Fig. 2(b), respectively. In both algorithms, no source depletes the battery and stops working. DSCC allocates the sampling rate more evenly among sources and time horizon, while the curves of source rate in QuickFix tightly follow the trend of the energy harvesting rate.

We also compare DSCC with the algorithm that the battery capacity is assumed to be unlimited, so the conservative case that the battery level reaches maximum and misses recharging opportunities is prohibitive. Based on DSCC, we can either set each source's battery capacity $\left\{B_i^{\max}\right\}_{i \in \mathcal{N}}$ to be sufficiently large, or set the Lagrangian multiplier $\boldsymbol{\Lambda}$ and missed energy $\boldsymbol{\Delta}$ to be zero (i.e., to relax the left half $\sum_{t=1}^h D_i^t\left(\boldsymbol{r}^t, \delta_i^t\right) \geq L_i^h$ of the battery capacity constraint (7)), to reach such an assumption. The revised algorithm is referred to as DSCC-with unlimited battery capacity (DSCC-un) and its simulation result is shown in Fig. 2(c). We see that the battery level can reach very high and DSCC-un flattens the curves of source rate as much as possible.

The performance of DSCC, QuickFix, and DSCC-un is numerically compared in TABLE III. We compare their network utility, total sampling rates, and total missed energy in five days from 2012 December 10 to 14. It shows that DSCC always

[3]The following figures are based on the solar data of December 12, 2012. We focus on the daytime since the energy harvesting rate is zero at night.

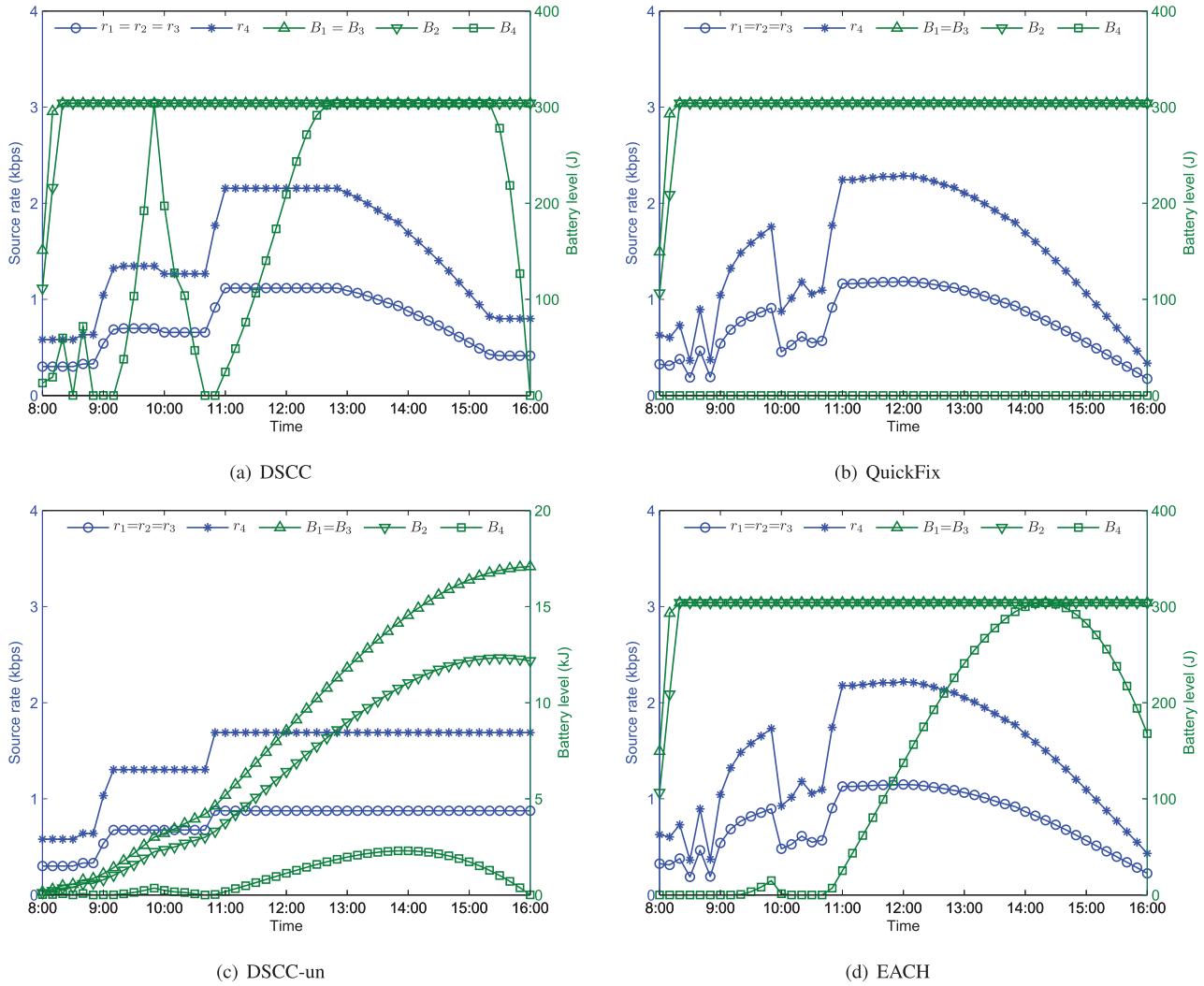

(a) DSCC

(b) QuickFix

(c) DSCC-un

(d) EACH

Fig. 2. Simulation results.

TABLE III
PERFORMANCE COMPARISON

Comparison metric \ 2012 December		10	11	12	13	14
Network utility $\sum_{h\in\mathcal{H}}\sum_{i\in\mathcal{N}} W\left(r_i^h\right)$	DSCC	-153	-27.8	-38.8	-195	-203
	QuickFix	-167	-41.3	-46.4	-206	-211
	DSCC-un	-139	-13.9	-31.1	-175	-201
Total sampling rates $\sum_{h\in\mathcal{H}}\sum_{i\in\mathcal{N}} r_i^h$ $(kbps)$	DSCC	104.3	198.0	183.2	107.6	77.98
	QuickFix	104.3	198.0	183.2	107.7	77.99
	DSCC-un	104.3	198.0	183.2	107.6	77.98
Total missed energy $\sum_{h\in\mathcal{H}}\sum_{i\in\mathcal{N}} \delta_i^h$ (kJ)	DSCC	25.12	49.02	45.24	26.44	18.79
	QuickFix	25.12	49.02	45.24	26.44	18.79
	DSCC-un	0	0	0	0	0

obtains higher network utility than QuickFix. This is because, for the logarithmic utility function, the flatter the curves of source rate, the higher the network utility. It is also observed that, all three algorithms have almost the same total sampling rates; however, DSCC-un can store all harvested energy due to unlimited battery capacity. Hence, it can flatten the curves of source rate as much as possible, and thereby obtains the best network utility. On the other hand, DSCC and QuickFix have almost the same total missed energy; however, by use of battery, DSCC can allocate the sampling rate more evenly among sources and time horizon, and thereby obtains higher network utility than QuickFix.

We finally compare DSCC with EACH [21], whose energy constraint is that the energy consumption rate does not exceed

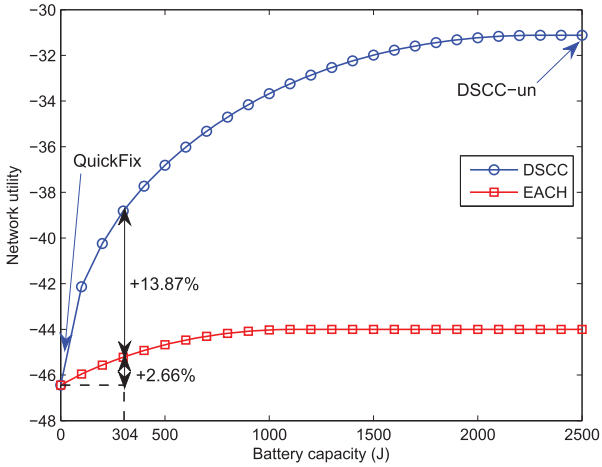

Fig. 3. Battery capacity impact on network utility.

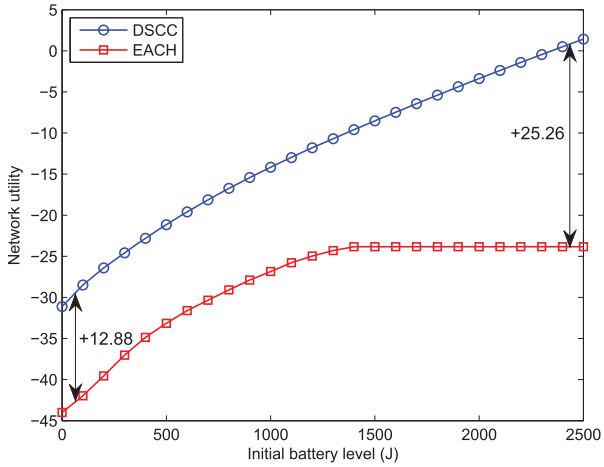

Fig. 4. Initial battery level impact on network utility.

the energy allocation. Although the energy allocation is based on the energy harvesting rate and current battery level, it is heuristically solved without considering the global optimality. The remaining problem, without the temporally-coupled part, is then similar to QuickFix. Although EACH improves the network utility a little bit, it still cannot obtain the globally optimal solution. The simulation result of EACH is shown in Fig. 2(d) and partly in Fig. 3. It can be seen that EACH improves the network utility by 2.66%, and DSCC improves it by 16.53% when the battery capacity is 304 J.

From the above, the proposed DSCC algorithm has better performance than the baseline approaches QuickFix and EACH. The underlying reason is that DSCC uses battery more efficiently from the global optimal view, such that the sampling rates are allocated more evenly among sources and time horizon; while the curves of source rate in QuickFix and EACH tightly follow the trend of the energy harvesting rate, either without consideration of battery or from the local optimal view. Therefore, DSCC improves the network utility of QuickFix and EACH by 16.53% and 13.87% respectively when the battery capacity is 304 J.

C. Battery Capacity and Initial Battery Level Impact

We first evaluate the impact of battery capacity on the network utility. QuickFix can be viewed as the algorithm with zero battery capacity, because its energy constraint is that the energy consumption rate does not exceed the energy harvesting rate. Without consideration of battery, such constraints are not coupling across the time horizon, making the problem easier to solve. However, since the excessive harvested energy is not considered to be stored in the battery for later usage, there is no flexibility to allocate the sampling rate evenly among sources and time horizon, and thus the network utility is low. On the contrary, DSCC-un is the algorithm with unlimited battery capacity, so it has the maximum flexibility to flatten the curves of source rate as much as possible, and hence the network utility is high. Finally, DSCC, with limited battery capacity, is the algorithm between these two. The impact of battery capacity on the network utility is shown in Fig. 3. We see that the network utility of DSCC and EACH increases with the battery capacity. Figure 3 also shows that their performance does not increase indefinitely with the battery capacity but reaches their saturation points when the battery capacity is over 2500 and 1000 J respectively. When the battery capacity is zero, DSCC corresponds to QuikFix. And when the battery capacity becomes large enough, DSCC is referred to as DSCC-un. It is also observed that, without battery, the network utility is the worst. No matter which algorithm (QuickFix, EACH, or DSCC) is applied, the results are the same. However, by use of battery, EACH improves the performance a little bit, but DSCC improves it much more and always outperforms EACH. The best network utility is achieved by DSCC-un, i.e., DSCC-with unlimited battery capacity.

We also evaluate the impact of initial battery level on the network utility. Note that in the above simulations, we have assumed that the initial battery level of each source is zero. Now we fix the battery capacity of each source at 2500 J, while vary their initial battery level from zero to full. The impact of initial battery level on the network utility is shown in Fig. 4. We can observe that the network utility of DSCC and EACH increases with the initial battery level. Figure 4 also shows that the performance of EACH does not increase indefinitely with the initial battery level but reaches a saturation point when the initial battery level is over 1500 J. The reason is because the EACH algorithm does not take the initial battery level into consideration. Therefore the curve for EACH flattens out after the initial battery level exceeds a threshold. When the initial battery level is zero, the network utility is the worst. But the network utility of DSCC is much better than that of EACH, because DSCC makes use of battery more efficiently. Besides, the network utility of DSCC increases with the initial battery level much faster than that of EACH. It is also seen that, when the initial battery is full, DSCC outperforms EACH most, where the outperformance of the network utility is almost twice of that when the initial battery is zero.

We finally evaluate the impact of both battery capacity and initial battery level on the network utility. We vary the battery capacity of each source from zero to 2500 J. While for each battery capacity, we also vary the initial battery level from

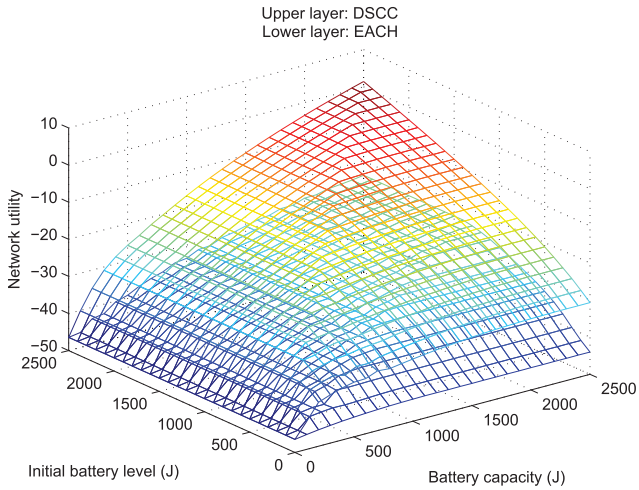

Fig. 5. Battery capacity and initial battery level impact on network utility.

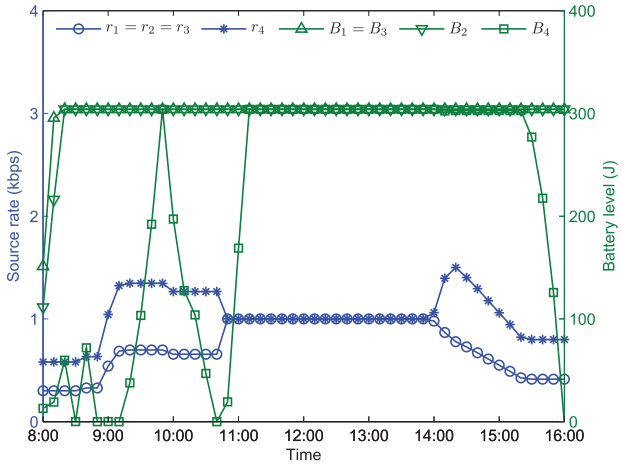

Fig. 6. DSCC under link capacity constraint.

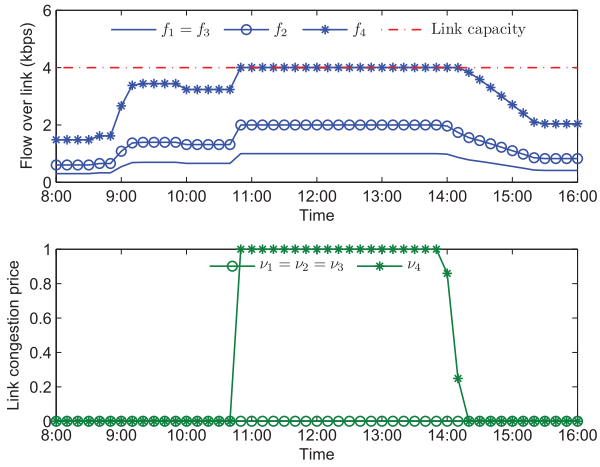

Fig. 7. Flow over link (top, solid), link capacity (top, dashed), and link congestion price (bottom).

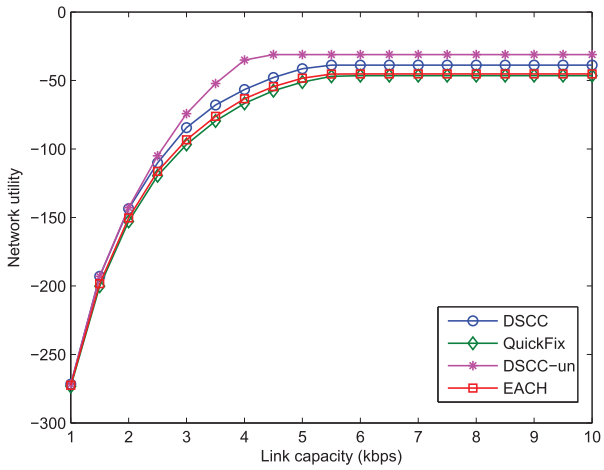

Fig. 8. Link capacity impact on network utility.

zero to full. The impact of both battery capacity and initial battery level on the network utility is shown in Fig. 5, where the upper layer is the performance of DSCC, and the lower layer for EACH. Note that in this figure, when the initial battery level is larger than the battery capacity, the corresponding result is set equally to that when the initial battery level is full. It can be seen that, when the battery capacity is zero, the network utility is the worst, despite of DSCC or EACH. The network utility increases with both the battery capacity and initial battery level. The best performance, for both DSCC and EACH, is achieved when the battery capacity is the largest and the initial batter level is full. In addition, DSCC always obtains higher network utility than EACH, under any battery capacity and any initial batter level. This is because DSCC uses battery more efficiently to allocate the sampling rate evenly among sources and time horizon, and thus achieves better performance.

D. Link Capacity Impact

Note that in the above simulations, we have assumed that the link capacity is large enough. Based on DSCC, we can either set all links' capacities $\{c_i^h\}_{i\in\mathcal{N}}$ to be sufficiently large, or set the link congestion price $\boldsymbol{N}$ to be zero (i.e., to relax the link capacity constraint (1)), to reach such an assumption. We first set each link's capacity at 4 *kbps* and see its impact on the algorithms. We take DSCC as an example, whose performance under the link capacity constraint is shown in Fig. 6, and the other three algorithms have the similar results. Compared with Fig. 2(a), we can observe that from 11:00 to 14:00, although the energy harvesting rate is high, the corresponding sampling rate is not accordingly increased, due to the link capacity constraint of the bottleneck link 4.

Specifically, for the DSCC algorithm under the link capacity constraint, the flow over link $f_i^h \triangleq r_i^h + \sum_{j\in\mathcal{A}(i)} r_j^h$ and the link congestion price ν_i^h are shown in Fig. 7. It is verified that the link capacity constraint (1) is satisfied, especially for the bottleneck link 4. It can be seen that the link congestion prices are zero whenever the link is un-congested. This is due to the complementary slackness condition $\nu_i^h\left(c_i^h - f_i^h\right) = 0$, which states that for all inactive constraints the corresponding Lagrangian multipliers should be zero.

To evaluate the impact of link capacity on the network utility, we fix the battery capacity of each source at 304 J (except for DSCC-un who has unlimited battery capacity) and their initial battery level is zero, while vary each link's capacity from

TABLE IV
COMPARISON BETWEEN DSCC AND YALMIP SOLUTIONS

Battery capacity (J)	Network utility		Initial battery level (J)	Network utility		Link capacity (K/s)	Network utility	
	DSCC	YALMIP		DSCC	YALMIP		DSCC	YALMIP
0	-44.78	-46.44	0	-31.12	-31.13	1	-271.71	-271.71
500	-36.82	-36.82	500	-21.16	-21.22	2	-143.61	-143.88
1000	-33.67	-33.68	1000	-14.17	-14.21	3	-84.48	-84.64
1500	-31.99	-32.00	1500	-8.52	-8.54	4	-56.63	-56.64
2000	-31.23	-31.24	2000	-3.37	-3.37	5	-41.42	-41.42
2500	-31.12	-31.13	2500	1.43	1.43	6	-38.77	-38.78

1 to 10 *kbps*. The impact of link capacity on the network utility is shown in Fig. 8. It is observed that the network utility increases with the link capacity. As aforementioned, QuickFix and DSCC-un indicate the lower and upper bounds respectively as benchmarks. EACH improves the lower baseline a little bit, but DSCC improves it much more and always outperforms EACH. Figure 8 also shows that the performance does not increase indefinitely with the link capacity but reaches their saturation points when the link capacity is over 5 or 6 *kbps*.

E. Optimality and Scalability

In this paper, we propose the DSCC algorithm to solve the problem (8) in a distributed fashion. As a nonlinear problem (NLP), it could be centrally solved through an NLP solver. To demonstrate the global optimality of the distributed algorithm, we compare the solution of DSCC with that of a centralized solver YALMIP [36]. We utilize YALMIP to solve the problem (8) with various parameter settings, which have covered all scenarios mentioned above. In TABLE IV we list a few sample solutions for comparison. The left column of solution is under the scenario that the battery capacity impacts on the network utility. The initial battery level of each source is zero, while their battery capacity varies from zero to 2500 J. The solution of DSCC is also shown in Fig. 3. The middle column of solution is under the scenario that the initial battery level impacts on the network utility. The battery capacity of each source is fixed at 2500 J, while their initial battery level varies from zero to full. The solution of DSCC is also shown in Fig. 4. The right column of solution is under the scenario that the link capacity impacts on the network utility. The battery capacity of each source is fixed at 2500 J and their initial battery level is zero, while each link's capacity varies from 1 to 6 *kbps*. The solution of DSCC is also shown in Fig. 8. It is observed that the DSCC and YALMIP solutions are almost the same, where the very small differences result from the error tolerance ε. Since DSCC can achieve almost the same results as a centralized solver, its global optimality is guaranteed. This is where our propose algorithm outperforms existing distributed approaches.

To investigate the scalability issue of the DSCC algorithm, we extend the above simulation to dense-deployed large-scale RSNs with more sources. The impact of source number on the iteration number and simulation time is shown in Fig. 9. We consider RSNs with the topology of full and complete binary trees, taking the sink as the root. That is, the source number is 2^{l+1}-2, which increases exponentially with the tree level l. We perform simulations on these binary trees to show the iteration

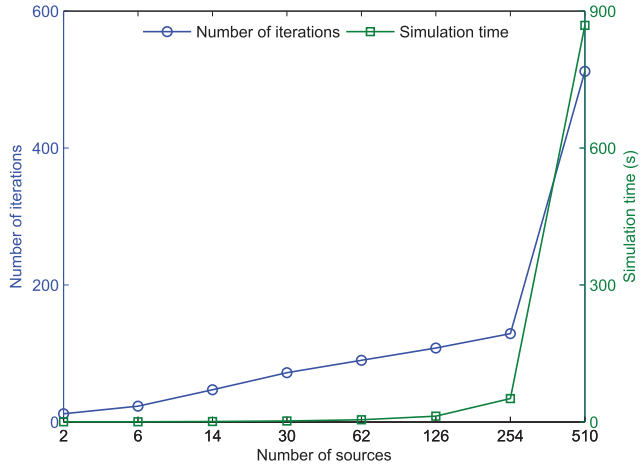

Fig. 9. Source number impact on iteration number and simulation time.

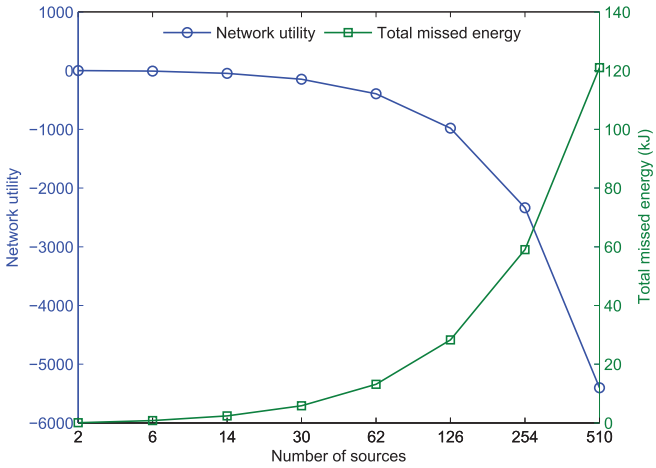

Fig. 10. Source number impact on network utility and total missed energy.

number and simulation time required for DSCC convergence. It can be observed that, as the source number increases exponentially, the iteration number also increases exponentially. Since the simulation time is dependent on the iteration number, the changing trend of the simulation time is similar. As the source number increases to more than 500, the proposed distributed algorithm consumes the simulation time of less than 900 s. Since the algorithm performs only once at the beginning of the time cycle (one day), the simulation time is acceptable. The impact of source number on the network utility and total missed energy is shown in Fig. 10. It is seen that, with the network scale expansion, the network utility decreases and the total missed energy increases. The reason is that, as the source

number increases, the burden on the bottleneck source (link) becomes heavier, but the harvested energy and link capacity of the bottleneck source (link) do not change. Therefore, more harvested energy will be missed and the network utility degrades.

VII. Conclusion and Future Work

In this paper, the NUM problem in static-routing RSNs with the link and battery capacity constraints has been fully investigated. The challenge lies in that the battery capacity constraint is spatiotemporally coupling, which cannot be directly tackled. We attempt to jointly optimize the sampling rate and battery level by carefully tackling the spatiotemporally-coupled link and battery capacity constraints. By means of dual decomposition, we decouple the original problem equivalently into separable subproblems, which can be locally solved in the context of joint rate and battery control. Based on this, we have proposed a distributed algorithm to obtain the globally optimal solution. Numerical results demonstrate that the proposed algorithm always achieves higher network utility than existing approaches. In addition, the impact of link/battery capacity and initial battery level on the network utility is further investigated.

For our future work, the NUM problem in dynamic-routing RSNs with the link and battery capacity constraints will be considered. In this context, flow rates will be the additional variables in the problem formulation to determine the optimal routing. Thus, the sampling rate, battery level, and routing strategy need to be jointly optimized. However, since the energy consumption rate for data transmitting will be dependent on the routing design and no longer fixed as in the static-routing case, the problem would become more complicated to solve.

References

[1] R. Deng, Y. Zhang, S. He, J. Chen, and X. Shen, "Globally optimizing network utility with spatiotemporally-coupled constraint in rechargeable sensor networks," in *Proc. IEEE Globecom*, 2013, pp. 5121–5126.

[2] J. Chen, W. Xu, S. He, Y. Sun, P. Thulasiraman, and X. Shen, "Utility-based asynchronous flow control algorithm for wireless sensor networks," *IEEE J. Sel. Areas Commun.*, vol. 28, no. 7, pp. 1116–1126, Sep. 2010.

[3] Y. Hu and A. Liu, "An efficient heuristic subtraction deployment strategy to guarantee quality of event detection for WSNS," *Comput. J.*, vol. 58, no. 8, pp. 1747–1762, 2015.

[4] J. Chen, Q. Yu, B. Chai, Y. Sun, Y. Fan, and X. Shen, "Dynamic channel assignment for wireless sensor networks: A regret matching based approach," *IEEE Trans. Parallel Distrib. Syst.*, vol. 26, no. 1, pp. 95–106, Jan. 2015.

[5] Y. Liu, A. Liu, and S. He, "A novel joint logging and migrating traceback scheme for achieving low storage requirement and long lifetime in WSNS," *AEU-Int. J. Electron. Commun.*, vol. 69, no. 10, pp. 1464–1482, 2015.

[6] J. Wang, Q. Gao, H. Wang, P. Cheng, and K. Xin, "Device-free localization with multidimensional wireless link information," *IEEE Trans. Veh. Technol.*, vol. 64, no. 1, pp. 356–366, Jan. 2015.

[7] H. Zhang, P. Cheng, L. Shi, and J. Chen, "Optimal DOS attack scheduling in wireless networked control system," *IEEE Trans. Control Syst. Technol.*, doi: 10.1109/TCST.2015.2462741, to be published.

[8] D. Dondi, A. Bertacchini, D. Brunelli, L. Larcher, and L. Benini, "Modeling and optimization of a solar energy harvester system for self-powered wireless sensor networks," *IEEE Trans. Ind. Electron.*, vol. 55, no. 7, pp. 2759–2766, Jul. 2008.

[9] S. He, J. Chen, F. Jiang, D. K. Yau, G. Xing, and Y. Sun, "Energy provisioning in wireless rechargeable sensor networks," *IEEE Trans. Mobile Comput.*, vol. 12, no. 10, pp. 1931–1942, Oct. 2013.

[10] Y. K. Tan and S. K. Panda, "Energy harvesting from hybrid indoor ambient light and thermal energy sources for enhanced performance of wireless sensor nodes," *IEEE Trans. Ind. Electron.*, vol. 58, no. 9, pp. 4424–4435, Sep. 2011.

[11] Y. K. Tan and S. K. Panda, "Optimized wind energy harvesting system using resistance emulator and active rectifier for wireless sensor nodes," *IEEE Trans. Power Electron.*, vol. 26, no. 1, pp. 38–50, Jan. 2011.

[12] T. J. Kazmierski, L. Wang, G. V. Merrett, B. M. Al-Hashimi, and M. Aloufi, "Fast design space exploration of vibration-based energy harvesting wireless sensors," *IEEE Sensors J.*, vol. 13, no. 11, pp. 4393–4401, Nov. 2013.

[13] O. Ozel, K. Tutuncuoglu, J. Yang, S. Ulukus, and A. Yener, "Transmission with energy harvesting nodes in fading wireless channels: Optimal policies," *IEEE J. Sel. Areas Commun.*, vol. 29, no. 8, pp. 1732–1743, Sep. 2011.

[14] C. Huang, R. Zhang, and S. Cui, "Throughput maximization for the Gaussian relay channel with energy harvesting constraints," *IEEE J. Sel. Areas Commun.*, vol. 31, no. 8, pp. 1469–1479, Aug. 2013.

[15] H. Dai, X. Wu, G. Chen, L. Xu, and S. Lin, "Minimizing the number of mobile chargers for large-scale wireless rechargeable sensor networks," *Comput. Commun.*, vol. 46, pp. 54–65, 2014.

[16] J. Chen, S. He, and Y. Sun, *Rechargeable Sensor Networks: Technology, Theory, and Application-Introducing Energy Harvesting to Sensor Networks*. Singapore: World Scientific, 2014.

[17] H. Dai, X. Wu, L. Xu, F. Wu, S. He, and G. Chen, "Practical scheduling for stochastic event capture in energy harvesting sensor networks," *Int. J. Sensor Netw.*, vol. 18, nos. 1–2, pp. 85–100, 2015.

[18] Y. Zhang, S. He, and J. Chen, "Data gathering optimization by dynamic sensing and routing in rechargeable sensor networks," *IEEE/ACM Trans. Netw.*, doi: 10.1109/TNET.2015.2425146, to be published.

[19] H. Dai, G. Chen, C. Wang, S. Wang, X. Wu, and F. Wu, "Quality of energy provisioning for wireless power transfer," *IEEE Trans. Parallel Distrib. Syst.*, vol. 26, no. 2, pp. 527–537, Feb. 2015.

[20] R. Liu, P. Sinha, and C. Koksal, "Joint energy management and resource allocation in rechargeable sensor networks," in *Proc. IEEE INFOCOM*, 2010, pp. 1–9.

[21] Y. Zhang, S. He, J. Chen, Y. Sun, and X. Shen, "Distributed sampling rate control for rechargeable sensor nodes with limited battery capacity," *IEEE Trans. Wireless Commun.*, vol. 12, no. 6, pp. 3096–3106, Jun. 2013.

[22] L. Wang *et al.*, "AdaptSens: An adaptive data collection and storage service for solar-powered sensor networks," in *Proc. IEEE Real-Time Syst. Symp. (RTSS)*, 2009, pp. 303–312.

[23] R. Liu, K. Fan, Z. Zheng, and P. Sinha, "Perpetual and fair data collection for environmental energy harvesting sensor networks," *IEEE/ACM Trans. Netw.*, vol. 19, no. 4, pp. 947–960, Aug. 2011.

[24] Z. Mao, C. E. Koksal, and N. B. Shroff, "Near optimal power and rate control of multi-hop sensor networks with energy replenishment: Basic limitations with finite energy and data storage," *IEEE Trans. Autom. Control*, vol. 57, no. 4, pp. 815–829, Apr. 2012.

[25] Y. Gu, L. He, T. Zhu, and T. He, "Achieving energy-synchronized communication in energy-harvesting wireless sensor networks," *ACM Trans. Embedded Comput. Syst.*, vol. 13, no. 2s, p. 68, 2014.

[26] Z. Li, Y. Peng, D. Qiao, and W. Zhang, "Joint charging and rate allocation for utility maximization in sustainable sensor networks," in *Proc. IEEE 11th Annu. Int. Conf. Sens. Commun. Netw. (SECON)*, 2014, pp. 459–467.

[27] D. K. Noh and K. Kang, "Balanced energy allocation scheme for a solar-powered sensor system and its effects on network-wide performance," *J. Comput. Syst. Sci.*, vol. 77, no. 5, pp. 917–932, 2011.

[28] S. Boyd and L. Vandenberghe, *Convex Optimization*. Cambridge, U.K.: Cambridge Univ. Press, 2004.

[29] D. Palomar and M. Chiang, "A tutorial on decomposition methods for network utility maximization," *IEEE J. Sel. Areas Commun.*, vol. 24, no. 8, pp. 1439–1451, Aug. 2006.

[30] S. He, J. Chen, D. K. Yau, and Y. Sun, "Cross-layer optimization of correlated data gathering in wireless sensor networks," *IEEE Trans. Mobile Comput.*, vol. 11, no. 11, pp. 1678–1691, Nov. 2012.

[31] R. Deng, Z. Yang, F. Hou, M.-Y. Chow, and J. Chen, "Distributed real-time demand response in multiseller–multibuyer smart distribution grid," *IEEE Trans. Power Syst.*, vol. 30, no. 5, pp. 2364–2374, Sep. 2015.

[32] R. Deng, G. Xiao, R. Lu, and J. Chen, "Fast distributed demand response with spatially-and temporally-coupled constraints in smart grid," *IEEE Trans. Ind. Informat.*, vol. 11, no. 6, pp. 1597–1606, Dec. 2015.

[33] N. Trichakis, A. Zymnis, and S. Boyd, "Dynamic network utility maximization with delivery contracts," in *Proc. IFAC World Congr.*, 2008, pp. 2907–2912.

[34] J. Polastre, R. Szewczyk, and D. Culler, "Telos: enabling ultra-low power wireless research," in *Proc. IEEE 4th Int. Symp. Inf. Process. Sensor Netw. (IPSN)*, 2005, pp. 364–369.
[35] A. Andreas and T. Stoffel, "Solar radiation research laboratory (SRRL): baseline measurement system (BMS)," NREL Tech. Rep. DA-5500-56488 [Online]. Available: http://dx.doi.org/10.5439/1052221
[36] J. Löfberg, "YALMIP: A toolbox for modeling and optimization in MATLAB," in *Proc. IEEE Int. Symp. Comput. Aided Control Syst. Des. (CACSD)*, 2004, pp. 284–289.

Ruilong Deng (S'11–M'14) received the B.Sc. and Ph.D. degrees in control science and engineering from Zhejiang University, Hangzhou, China, in 2009 and 2014, respectively. He was a Visiting Scholar at Simula Research Laboratory, Fornebu, Norway, in 2011, and the University of Waterloo, Waterloo, ON, Canada, from 2012 to 2013. He was a Research Fellow with Nanyang Technological University, Singapore, from 2014 to 2015. Currently, he is an AITF Postdoctoral Fellow with the Department of Electrical and Computer Engineering, University of Alberta, Edmonton, AB, Canada. His research interests include smart grid, cognitive radio, and wireless sensor network. He currently serves as an Editor for IEEE/KICS JOURNAL OF COMMUNICATIONS AND NETWORKS, and a Guest Editor for IEEE TRANSACTIONS ON EMERGING TOPICS IN COMPUTING.

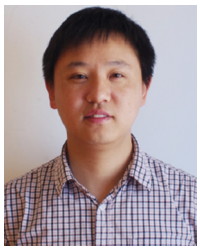

Yongmin Zhang (S'12–M'15) received the Ph.D. degree in control science and engineering from Zhejiang University, Hangzhou, China, in 2015. From November 2013 to June 2014, he was a Visiting Scholar at the California Institute of Technology, Pasadena, CA, USA. Currently, he is a member of the Group of Networked Sensing and Control and a Postdoctoral Research Fellow with the State Key Laboratory of Industrial Control Technology, Zhejiang University. His research interests include wireless sensor networks and smart grid. He currently serves as a Guest Editor for *Peer-to-Peer Networking and Applications*.

Shibo He (M'13) received the Ph.D. degree in control science and engineering from Zhejiang University, Hangzhou, China, in 2012. He is currently a Professor with Zhejiang University. He was an Associate Research Scientist from March 2014 to May 2014, and a Postdoctoral Scholar from May 2012 to February 2014, with Arizona State University, Tempe, AZ, USA. From November 2010 to November 2011, he was a Visiting Scholar at the University of Waterloo, Waterloo, ON, Canada. His research interests include wireless sensor networks, crowd sensing, and big data analysis. He serves on the Editorial Board of *Springer Peer-to-Peer Networking and Application* and *KSII Transactions on Internet and Information Systems*, and is a Guest Editor of *Elsevier Computer Communications* and *Hindawi International Journal of Distributed Sensor Networks*.

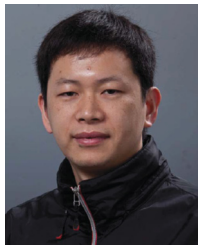

Jiming Chen (M'08–SM'11) received the B.Sc. and Ph.D. degrees in control science and engineering from Zhejiang University, Hangzhou, China, in 2000 and 2005, respectively. He was a Visiting Researcher at INRIA in 2006, National University of Singapore, Singapore, in 2007, and University of Waterloo, Waterloo, ON, Canada, from 2008 to 2010. Currently, he is a Full Professor with the College of Control Science and Engineering, and the coordinator of the Group of Networked Sensing and Control with the State Key Laboratory of Industrial Control Technology and Vice Director of the Institute of Industrial Process Control, Zhejiang University. His research interests include sensor networks and networked control. He currently serves as Associate Editor for several international journals including the IEEE TRANSACTIONS ON PARALLEL AND DISTRIBUTED SYSTEM, the IEEE TRANSACTIONS ON INDUSTRIAL ELECTRONICS, the IEEE NETWORK, and the IEEE TRANSACTIONS ON CONTROL OF NETWORK SYSTEMS. He was a Guest Editor of the IEEE TRANSACTIONS ON AUTOMATIC CONTROL.

Xuemin (Sherman) Shen (M'97–SM'02–F'09) received the B.Sc. degree from Dalian Maritime University, Dalian, China, in 1982, and the M.Sc. and Ph.D. degrees from Rutgers University, New Brunswick, NJ, USA, in 1987 and 1990, respectively, all in electrical engineering. He is a Professor and the University Research Chair of the Department of Electrical and Computer Engineering, University of Waterloo, Waterloo, ON, Canada, where he has served the Associate Chair for Graduate Studies from 2004 to 2008. His research interests include resource management in interconnected wireless/wired networks, wireless network security, social networks, smart grid, and vehicular ad hoc and sensor networks. He is a Royal Society of Canada Fellow, an Engineering Institute of Canada Fellow, a Canadian Academy of Engineering Fellow, and a Distinguished Lecturer of the IEEE Vehicular Technology Society and Communications Society. He is an elected member of the IEEE Computer Society Board of Governors, and the Chair of the Distinguished Lecturers Selection Committee. He is a Registered Professional Engineer of ON. He serves/served as the Editor-in-Chief for the IEEE NETWORK, *Peer-to-Peer Networking and Application*, and *IET Communications*; a Founding Area Editor for the IEEE TRANSACTIONS ON WIRELESS COMMUNICATIONS; an Associate Editor for the IEEE TRANSACTIONS ON VEHICULAR TECHNOLOGY, *Computer Networks*, and *ACM/Wireless Networks*; and a Guest Editor for the IEEE JOURNAL ON SELECTED AREAS IN COMMUNICATIONS, the IEEE WIRELESS COMMUNICATIONS, the *IEEE Communications Magazine*, and *ACM Mobile Networks and Applications*. He was the recipient of the Excellent Graduate Supervision Award in 2006 and the Outstanding Performance Award in 2004, 2007, 2010, and 2014 from the University of Waterloo; the Premier's Research Excellence Award in 2003 from the province of ON; and the Distinguished Performance Award in 2002 and 2007 from the Faculty of Engineering, University of Waterloo.